

# A Dual-Mode Beam Waveguide Resonator and Frequency Stabilizer at Millimeter-Wave Frequencies

J. W. MINK, MEMBER, IEEE, AND E. H. SCHEIBE, SENIOR MEMBER, IEEE

**Abstract**—By applying perturbation theory to one of the higher modes that may exist in the beam waveguide resonator (also known as the focused Fabry-Perot interferometer), it can be shown that the degeneracy of the mode system can be reduced, resulting in two mode systems with slightly different resonant frequencies. Using this result, a dual-mode frequency discriminator was constructed and used as a reference element for stabilizing the frequency of microwave sources. The stability of a 34-GHz stabilized source was better than 1 part in  $5 \times 10^7$  short term and better than 1 part in  $1.5 \times 10^6$  long term. The frequency sensitivity of this dual-mode resonator to changes in the properties of the dielectric medium between the end plates was utilized to determine the dielectric constant of gases at 34 GHz with an accuracy of a few parts in  $10^7$ .

## INTRODUCTION

THIS PAPER is concerned with only one of the many possible applications of the beam waveguide resonator as a useful circuit component in a millimeter-wave system. The beam waveguide resonator is an open structure consisting of two properly shaped reflecting plates separated by many wavelengths, as shown in Fig. 1. Deliberate and controlled dual-mode operation of the resonator, which is the basis for the useful applications presented here, was studied in some detail. The study was undertaken when it was found that an inadvertent distortion in the resonator resulted in dual-mode operation.

The mode system in the beam waveguide resonator

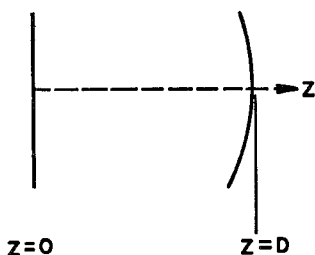


Fig. 1. Beam waveguide resonator.

Manuscript received October 22, 1965; revised January 17, 1966. The work reported in this paper was sponsored by the U. S. Army Electronic Research and Development Laboratory, Fort Monmouth, N. J., under Contract DA-36-039-sc-85188.

J. W. Mink is with the U. S. Army Electronics Command, Institute for Exploratory Research, Fort Monmouth, N. J. He was formerly with the Department of Electrical Engineering, University of Wisconsin.

E. H. Scheibe is with the Department of Electrical Engineering, University of Wisconsin, Madison.

with spherical reflectors is the same as that of the lens-type beam waveguide. A brief description of the mode system is necessary in order to understand the dual-mode operation of the resonator.

The mode system of the beam waveguide may be approximated by the following complete set of orthogonal functions [1]–[3]. These ideal field distributions are useful for the first few modes if the apertures are large compared with the operating wavelength.

$$E_{xnv} = \sqrt{\frac{\mu}{\epsilon}} H_{y nv} = A_{nv} (1 + u^2)^{-1/2} \left( \frac{\rho}{\rho_z} \right)^v L_n^v \left( \frac{\rho}{\rho_z} \right)^2 \cdot e^{-[1/2(\rho/\rho_z)^2 + j\psi]} \begin{Bmatrix} \cos v\phi \\ \sin v\phi \end{Bmatrix} \quad (1)$$

or

$$E_{y nv} = -\sqrt{\frac{\mu}{\epsilon}} H_{x nv} = A_{nv} (1 + u^2)^{-1/2} \left( \frac{\rho}{\rho_z} \right)^v L_n^v \left( \frac{\rho}{\rho_z} \right)^2 \cdot e^{-[1/2(\rho/\rho_z)^2 + j\psi]} \begin{Bmatrix} \cos v\phi \\ \sin v\phi \end{Bmatrix} \quad (1)$$

where

$x, y, z$  refer to the  $x$ -,  $y$ -,  $z$ -axis of a rectangular coordinate system

$n = 0, 1, 2, \dots; v = 0, 1, 2, \dots$

$L_n^v$  = Laguerre polynomial of degree  $n$  and order  $v$

$\phi$  = polar angle

$\psi = kz - (2n + v + 1) \tan^{-1} u + \frac{1}{2}(\rho/\rho_z)^2$

$u = z/k\rho_0^2$

$\lambda$  = free-space wavelength

$k = 2\pi/\lambda$

$\rho$  = radial coordinate  $\sqrt{x^2 + y^2}$

$\rho_z^2 = \rho_0^2(1 + u^2)$

and  $\rho_0$  is a mode set parameter determined by the focal length of the lenses and their separation, and may be expressed as follows:

$$\rho_0 = \frac{\sqrt{(2 - D/f)Df}}{k} \quad (2)$$

where  $f$  = focal length of paraboloidal phase corrector, and  $D$  = separation between phase correctors.

It is desirable when working with the beam waveguide or beam waveguide resonator to have a compact notation to designate each of the beam waveguide modes, and therefore a convenient and meaningful mode designation has been devised. An inspection of (1) shows that the mode field distribution is a product of two independent terms. One of these terms contains the radial amplitude distribution and is characterized by the Laguerre polynomial  $L_n^v$ . The other contains the angular dependence and is characterized by either  $\sin v\phi$  or  $\cos v\phi$ . The polarization of the electric field is also needed to completely specify any particular mode. A beam mode can be identified by the symbol

$$_x L_n^v \begin{pmatrix} \cos v\phi \\ \sin v\phi \end{pmatrix}.$$

The subscript  $n$  indicates the degree and the superscript  $v$  indicates the order of the Laguerre polynomial associated with the mode radial field distribution. The second subscript  $x$  may be either  $x$  or  $y$  and indicates the direction of polarization of the transverse electric field. The quantity within the parentheses represents the cyclic variations of the field in the  $\phi$  direction, and also indicates the positions of its maximums and minimums. Thus for a given  $n$  and  $v$ , two modes, one having a  $\cos v\phi$  variation and the other having a  $\sin v\phi$  variation, can exist for each of the two possible directions of polarization. The mode system is thus four times degenerate, except in the case where  $v$  equals zero where the modes differ only in polarization.

Furthermore from (1) it can be seen that each mode, as determined by  $n$  and  $v$ , has a plane phase surface at  $z=0$ . At any other distance  $z$  along the beam waveguide, the  $\rho$  independent part of the phase shift is

$$\tilde{\psi} = kz - (2n + v + 1) \tan^{-1} u \quad (3)$$

and is dependent only upon the particular mode of interest. The  $\rho$  dependent part of the phase shift is

$$\tilde{\psi} \approx \frac{1}{2} u \left( \frac{\rho}{\rho_z} \right)^2 \quad (4)$$

and is independent of the mode.

#### THEORY OF THE DUAL-MODE BEAM WAVEGUIDE RESONATOR

A resonator based on the beam waveguide transmission line is formed by placing across the beam a pair of conducting surfaces which serve as resonator end plates, and which are shaped to coincide with the phase fronts of the beam at the points of placement. The condition for resonance is that the phase shift of a wave progressing from one conducting surface to the other must be a multiple of  $\pi$ . A beam waveguide resonator with one conducting surface or end plate at the plane  $z=0$  and the other end plate separated a distance  $D$  from it is shown in Fig. 1. For a confocal resonator the

end plate at  $z=D$  has a paraboloidal shape whose focal length is  $D$ .

A resonator (such as shown in Fig. 1) operating at a frequency near 9.3 GHz was adjusted to resonate the  $L_0^1$  mode in order to measure its diffraction loss and to study its cross-sectional field distribution. The  $L_0^0$  mode, which is the lowest loss mode in the resonator (or beam waveguide), must be suppressed if the  $L_0^1$  mode is to survive in the resonator. This was accomplished in two ways. First, an inspection of (3) shows that there is a  $\pi/2$  radian phase shift between the  $L_0^0$  and  $L_0^1$  modes; hence, if the length of the resonator is adjusted for the  $L_0^1$  mode to resonate, the  $L_0^0$  mode will be discriminated against since it will not be resonant. Second, the radial field distribution as given by the Laguerre polynomial is a maximum on the axis for the  $L_0^0$  mode but is zero here for the  $L_0^1$  mode. The maximum for the  $L_0^1$  mode occurs at a radial distance from the axis, which corresponds to the radius where the  $L_0^0$  mode has decreased to  $e^{-1}$  of its maximum value. Therefore, if the coupling apertures are placed at this radius, the coupling to the  $L_0^1$  mode will be stronger than the coupling to the  $L_0^0$  mode. A lossy material may be placed on the axis of the resonator to further suppress the  $L_0^0$  mode with a very small effect on the  $L_0^1$  mode since the fields of the  $L_0^1$  mode are zero on the axis.

The response obtained for this resonator as a function of frequency is shown in Fig. 2. The  $L_0^0$  mode was effectively suppressed, but the double-hump response shown in Fig. 2 was unexpected. Except for the lowest loss mode ( $L_0^0$ ), the modes of the beam waveguide are four times degenerate, and the response shown in Fig. 2 can be explained only if the degeneracy of the system of modes has been reduced, perhaps because of a perturbation in the resonator. Upon close inspection it was found that the radii of curvature along the two principal axes of the paraboloidal end plate were different, thus a distortion or perturbation was indeed present.

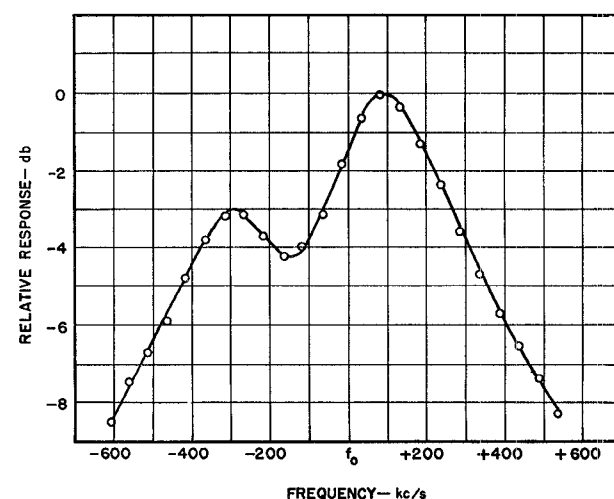


Fig. 2. Higher mode response of resonator.

The amplitude distribution of the  $L_0^1$  modes is given by (1), and is of the following form:

$$E_{x0_1} = \sqrt{\frac{\mu}{\epsilon}} H_{y0_1} = E_0 \left( \frac{\rho}{\rho_z} \right) L_0^1 \left( \frac{\rho}{\rho_z} \right)^2 \cdot e^{-1/2(\rho/\rho_z)^2} \begin{cases} \cos \phi \\ \sin \phi \end{cases}$$

$$E_{y0_1} = -\sqrt{\frac{\mu}{\epsilon}} H_{x0_1} = E_0 \left( \frac{\rho}{\rho_z} \right) L_0^1 \left( \frac{\rho}{\rho_z} \right)^2 \cdot e^{-1/2(\rho/\rho_z)^2} \begin{cases} \cos \phi \\ \sin \phi \end{cases}. \quad (5)$$

In Fig. 3 the field distribution of the  $yL_0^1$  ( $\sin \phi$ ) mode is shown in dotted lines, and the field distribution of the  $xL_0^1$  ( $\cos \phi$ ) mode is shown in solid lines. It is evident from (5) that the various  $L_0^1$  modes have symmetry with respect to the principal axes ( $x$  and  $y$ ) of the resonator end plates. The distortion found to exist in the curved end plates is also symmetrical with respect to these same axes, and hence the modes do not become coupled through the perturbation. Instead, the distortion has the effect of increasing the length of the resonator for the ( $\cos \phi$ ) mode and decreasing the length of the resonator for the ( $\sin \phi$ ) mode. This change of length for each of the two  $L_0^1$  modes results in two different resonant frequencies as shown in the response obtained in Fig. 2. This explanation of the behavior of the resonator can be substantiated theoretically using perturbation techniques. It can also be verified experimentally.

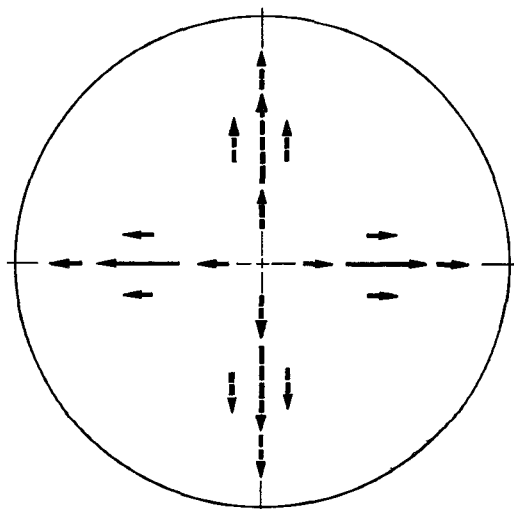


Fig. 3. Field pattern for  $L_0^1$  modes.

A paraboloid of revolution can be expressed as two sections of parabolic cylinders superimposed with their axes perpendicular to each other. Assume that the curvature of each parabolic cylinder deviates from the average curvature  $d$  by an amount  $\pm \Delta d$ . An equation for the surface can now be formulated as follows:

$$z = \rho^2 d + (x^2 - y^2) \Delta d \quad (6)$$

where

$$\rho^2 = x^2 + y^2$$

$$d = \frac{1}{4f_0}$$

$$\Delta d \simeq \frac{\Delta f}{4f_0^2}$$

$f_0$  = average focal length of parabola.

For small perturbations the following equation (derived in [4]) holds:

$$\frac{\omega - \omega_0}{\omega_0} = \frac{\int_{\Delta v} (\mu |H_T|^2 - \epsilon |E_T|^2) dv}{\int_v (\mu |H_T|^2 + \epsilon |E_T|^2) dv} \quad (7)$$

where

$\omega_0$  = resonant angular frequency of resonator

$\omega$  = any angular frequency near  $\omega_0$

$\Delta v$  = change of resonator volume due to deformation

and  $E_T$  and  $H_T$  are the total unperturbed transverse fields in the resonator.

Equation (7) was derived for closed cavities; however, the error involved in using it for an open beam waveguide resonator is very small. This error is of the order of the diffraction loss of the beam waveguide since the derivation of (7) does not take into account energy lost by diffraction.

The boundary conditions at the surface of the paraboloid require that the tangential electric field be zero because the surface is assumed to be a perfect conductor. Although the term involving  $|E_T|^2$  in the numerator of (7) is not zero, it is very small compared with the term involving  $|H_T|^2$  because  $H_T$  is near its maximum value throughout  $\Delta v$  while  $E_T$  is very small throughout  $\Delta v$ . The denominator of (7) is a measure of the total energy stored in the resonator. At resonance equal energies are stored in the magnetic and electric fields, and hence the total energy will be just twice the energy stored in one of the fields. Therefore, (7) can be expressed in terms of the magnetic field alone, and becomes

$$\frac{\omega - \omega_0}{\omega_0} = \frac{\int_{\Delta v} \mu |H_T|^2 dv}{2 \int_v \mu |H_T|^2 dv}. \quad (8)$$

The total magnetic field as given by (5) for one of the modes, the  $L_0^1$  ( $\cos \phi$ ) mode, may be written as

$$H_T = H_0 \left( \frac{\rho}{\rho_z} \right) e^{-1/2(\rho/\rho_z)^2} \cos \phi. \quad (9)$$

Introducing (6) and (9) into the numerator of (8) and performing the indicated integration yields

$$\int_{\Delta v} \mu |H_T|^2 dv = H_0^2 \frac{2\mu\pi\Delta d D^2}{k^2}. \quad (10)$$

In a practical beam waveguide resonator the field amplitude at the edges of the reflectors is extremely small, therefore the error introduced by allowing the radius of the reflectors to become infinite is less than 4 percent. The result given in (10) neglects the finite size of the reflectors. Introducing (9) into the denominator of (8) and performing the indicated integration yields

$$2 \int_v \mu |H_T|^2 dv = H_0^2 \frac{\pi\mu D^2}{k}. \quad (11)$$

Therefore, (8) becomes

$$\frac{\omega - \omega_0}{\omega_0} = \frac{2\Delta d}{k}. \quad (12)$$

If the preceding analysis is also applied to the  $L_0^1 (\sin \phi)$  mode, the result is

$$\frac{\omega - \omega_0}{\omega_0} = -\frac{2\Delta d}{k}. \quad (13)$$

Thus, the resonant frequency of each pair of modes is shifted from the unperturbed resonant frequency by an equal amount but in opposite directions. Hence, the degeneracy has been reduced from a four times degeneracy to a two times degeneracy. Equations (12) and (13) have been verified experimentally [5] at a frequency of 9 GHz. The expected change of the resonant frequency was 150 kHz while the measured change of the resonant frequency was 175 kHz. The agreement was considered to be quite good since for this case the perturbation was in the form of a distortion of the surface which could not be accurately controlled.

A perturbation can also be introduced into the beam waveguide resonator in the form of two small conducting pins placed on the  $x$ -axis of one of the end plates. One pin is placed on each side of center where the field intensity is a maximum for the  $L_0^1 (\cos \phi)$  mode. Thus from (1) it can be seen that this distortion will have a maximum effect on the  $L_0^1 (\cos \phi)$  mode and an extremely small effect on the  $L_0^1 (\sin \phi)$  mode since the perturbation occurs on a nodal line of the latter mode. For small perturbations the resonant frequency of the  $L_0^1 (\sin \phi)$  is assumed unchanged.

This type of perturbation has been found to be just as effective in reducing the degeneracy of  $L_0^1$  modes as the distorted end plate discussed previously. This latter type of perturbation has the advantage of ease of adjustment.

The foregoing analysis indicates that two uncoupled modes may exist in the beam waveguide resonator simultaneously. Also, their resonant frequencies may be separated by an amount determined by the type and extent of the perturbation introduced into the system as indicated by (12) and (13).

If the  $xL_0^1 (\cos \phi)$  mode as well as the  $yL_0^1 (\sin \phi)$  mode

is excited, and if the output of each mode is separately detected, the response of the resonator will be as shown in Fig. 4(a) where response  $A$  is for the  $yL_0^1 (\sin \phi)$  mode and response  $B$  is for the  $xL_0^1 (\cos \phi)$  mode. One mode is polarized in the  $x$  direction and the other mode is polarized in the  $y$  direction to obtain maximum isolation between the modes of the dual-mode beam waveguide resonator. Taking the difference between the detected outputs results in the overall response of the dual-mode beam waveguide resonator shown in Fig. 4(b). The behavior shown in Fig. 4(b) is that of a frequency discriminator, and hence such a resonator can be used as a control element in millimeter-wave systems.

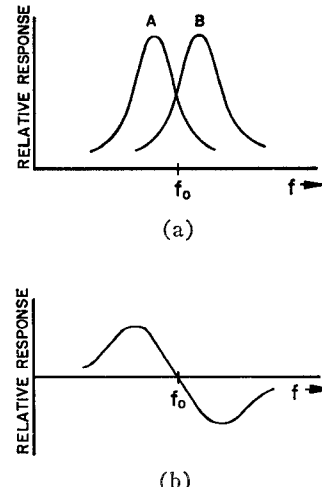


Fig. 4. Response of dual-mode resonator.

#### PERTURBATION THEORY: EXPERIMENTAL RESULTS

A dual-mode beam waveguide resonator was designed and constructed with the following parameters. The operating frequency was chosen to be near 33.75 GHz. In order to insure that the beam modes will be established, the radius of the reflecting end plates was chosen to be 10 cm, which is equal to about 11.2 wavelengths. The separation of the end plates was 57 cm, which was also the focal length of the paraboloidal phase-correcting end plate. A rigid frame was constructed to support the reflecting end plates and to allow one of the end plates to be moved to adjust the length of the resonator. The flat plate was clamped and then distorted by properly placed screws to obtain the desired perturbation. The resonator was adjusted to give the best discriminator response which occurred with a mode separation of about 500 kHz. The loaded  $Q$  of the resonator was about 75 000. A photograph of the resonator is shown in Fig. 5.

The output of the resonator was obtained from two properly placed and properly oriented crystal detectors located in the flat plate of the beam waveguide resonator. Each of the detectors must be arranged to be responsive to only one of the two modes present in the resonator. In practice, one was sensitive only to vertical

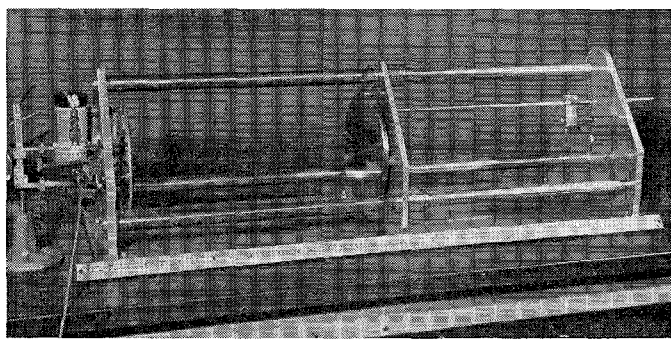


Fig. 5. 35-GHz beam waveguide resonator.

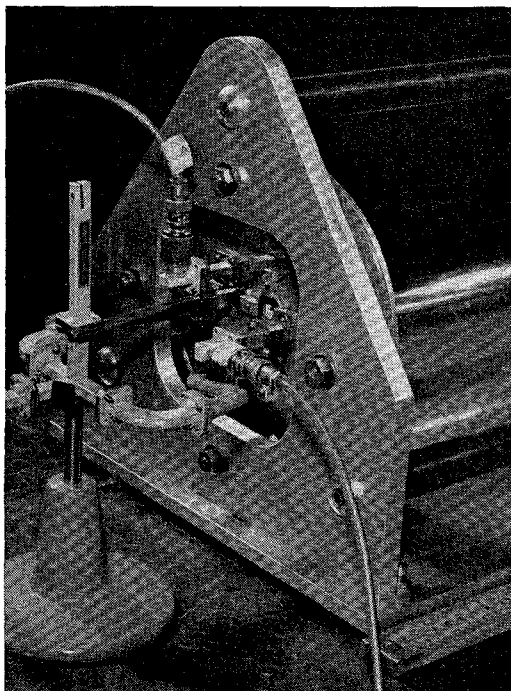


Fig. 6. 35-GHz resonator dual-mode coupling arrangement.

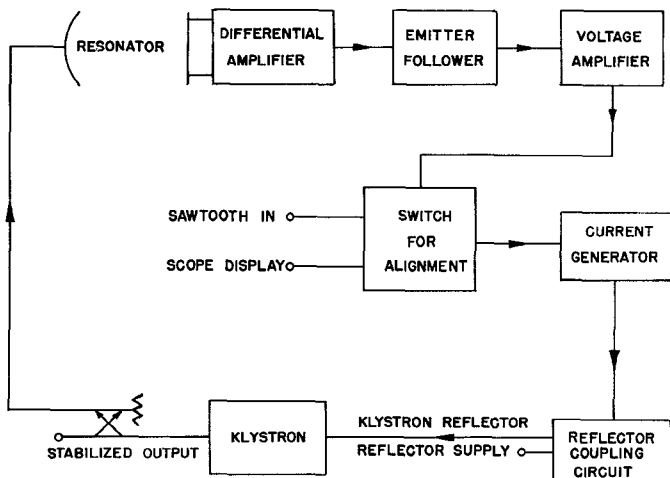


Fig. 7. Block diagram of final stabilization system.

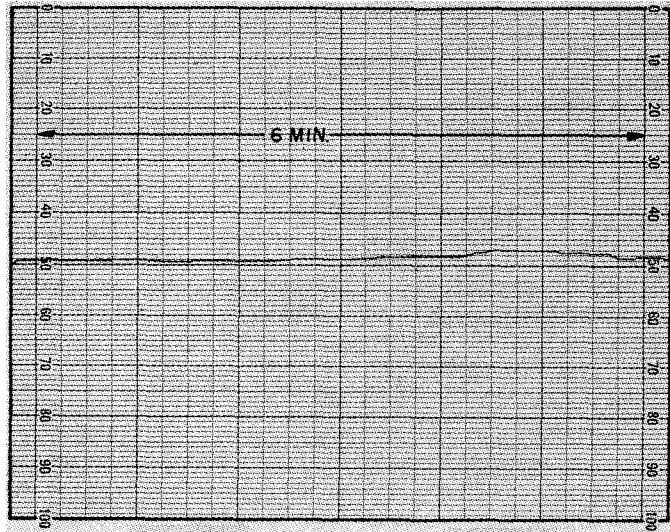


Fig. 8. Short-term frequency stability (1 kc/s per division).

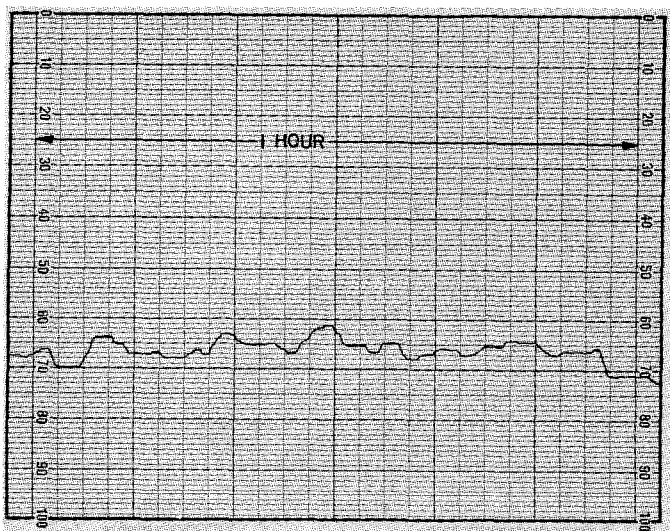


Fig. 9. Long-term frequency stability (2 kc/s per division).

polarization and the other to horizontal polarization in agreement with the polarizations shown in Fig. 3. The detectors were placed in the high field region of the  $L_0^1$  mode which occurs at a position corresponding to  $\rho = \rho_0$  or, for the actual resonator being discussed,  $\rho = 2.86$  cm. One detector was placed on the horizontal principal diameter and the other on the vertical principal diameter. Thus for either one of the detectors, the undesired mode will have both the wrong polarization and a nodal line at the detector. Therefore, this arrangement of detectors provides a minimum of cross coupling in the detected outputs. The input coupling was obtained by placing a waveguide on the same principal axis as its associated detector but on the opposite side of the center of the end plate. The polarization of each of the input waveguides corresponds to the polarization of its corresponding output waveguide. The details of the input and output coupling arrangement for the dual-mode beam waveguide resonator are shown in Fig. 6.

The discriminator response of the dual-mode beam waveguide resonator as shown in Fig. 4(b) can be used as a frequency reference in a frequency-stabilizing circuit for a backward wave tube or a reflex klystron. A block diagram of such a system for a reflex klystron is shown in Fig. 7. An analysis of this system will not be given here since it can be found in the literature [6]. The amplifier employed was transistorized and operated from batteries in order to reduce hum problems. The dc gain of the amplifier was 7500 with a dynamic output voltage range of  $\pm 30$  volts. The output of the amplifier was floating so that it could be connected in series with the klystron reflector circuit.

The stability of the stabilized oscillator was measured by comparing its output frequency with the frequency of an accurately known and very stable marker frequency. The marker frequency used has a quoted stability of 1 part in  $10^9$  per day. Recordings of both short-term and long-term stability were made and are shown in Figs. 8 and 9, respectively. The short-term stability (Fig. 8) averaged over a 6-minute period is approximately 0.415 kc/s per minute or better than 1 part in  $5 \times 10^7$ . The long-term stability (Fig. 9) is 20 kc/s per hour or better than 1 part in  $1.5 \times 10^6$ . The steps shown on the recordings in Figs. 8 and 9 indicate 1-second averages of frequency and are a measure of the frequency response of the recorder.

#### APPLICATIONS OF THE STABILIZED SYSTEM

While making the foregoing stability measurements it was noted that the stabilized oscillator frequency was very sensitive to turbulence of the medium in the resonator. This behavior suggests the possibility of using the resonator to measure the dielectric constant of a gas. The relative dielectric constant of a gas can be calculated by noting the difference between the resonant frequency of a resonator when it is evacuated and when it contains a gas. It is easy to show that for  $\epsilon_r$  close to unity

TABLE I  
DIELECTRIC CONSTANT OF GASES AT 34 GHz

Pressure mm Hg	$(\epsilon_r - 1) \times 10^6$ at 20°C				
	Air	He	N <sub>2</sub>	O <sub>2</sub>	A
0	0.0	0.0	0.0	0.0	0.0
100	68.3	9.5	70.5	63.9	66.3
200	137.9	18.2	140.2	127.1	131.6
300	208.0	26.0	210.8	189.8	197.9
400	277.9	34.7	281.7	254.6	264.8
500	347.8	42.6	352.7	317.3	331.6
600	417.6	50.4	423.2	380.8	397.8
700	487.5	58.4	493.8	444.1	465.1
760	530.1	63.2	537.4	484.9	504.5
800	557.4	66.5	564.8	508.9	530.7

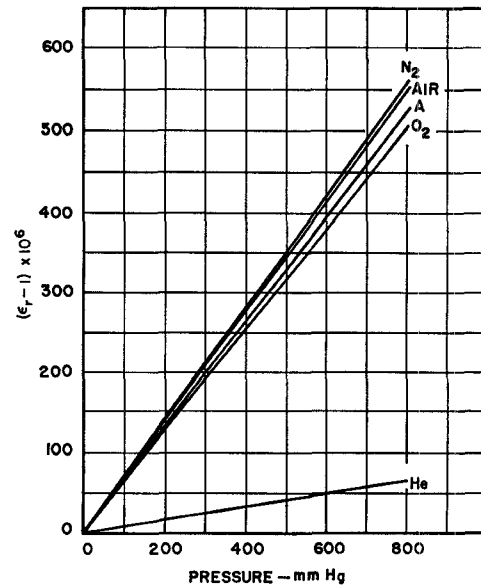


Fig. 10. Dielectric constant of gases vs. pressure.

$$\epsilon_r = 1 + 2 \frac{\Delta f}{f_0} \quad (17)$$

where  $f_0$  = resonant frequency of resonator in a vacuum, and  $\Delta f$  = difference in resonant frequency of the resonator when it is evacuated and when it contains a gas at a given pressure.

With the dual-mode beam waveguide resonator suspended at only two points in a sealed chamber, the relative dielectric constant  $\epsilon_r$  vs. pressure was determined for various gases. The results of these measurements<sup>1</sup> for air, helium, oxygen, nitrogen, and argon are given in Table I and in Fig. 10. The accuracy of these measurements is a few parts in  $10^7$ . A desirable feature of this method for measuring  $\epsilon_r$  is that the data for any one gas vs. pressure plots as a straight line, as shown in Fig. 10. Therefore, the value of  $\epsilon_r$  at atmospheric pressure can be determined with good accuracy. It appears that with refinements in the system, particularly an im-

<sup>1</sup> The measured values are in good agreement with other published results. See Maryott and Buckley [7], for example.

proved differential amplifier, the accuracy of this method of measurement could be increased by an order of magnitude.

Other uses of this system could be  $Q$  measurements at millimeter-wave frequencies, thickness measurements of dielectric sheets, or dielectric constant measurements of known thickness sheets. This system has the further advantage that it may be used over the entire millimeter-wave spectrum by changing only the source and detectors to respond to the desired frequency.

#### ACKNOWLEDGMENT

The authors wish to express their appreciation to Dr. G. Goubau and his staff at the U. S. Army Electronics Command, Fort Monmouth, N. J., for their most helpful suggestions and sincere cooperation during all phases of this investigation. They also wish to thank A. Murphy who assisted in the dielectric constant measurements, and R. Langdon who performed the

special machine operations involved in the construction of the apparatus.

#### REFERENCES

- [1] G. Goubau, "Optical relations for coherent wave beams," presented at 1962 Symposium on Electromagnetic Theory and Antennas, Copenhagen, Denmark. Published in *Electromagnetic Theory and Antennas* (International Series of Monographs on Electromagnetic Waves, vol. 6, pt. 2), E. C. Jordan, Ed. New York: Pergamon, 1963.
- [2] G. Goubau and F. Scherwing, "On the guided propagation of electromagnetic wave beams," *IRE Trans. on Antennas and Propagation*, vol. AP-9, pp. 248-256, May 1961.
- [3] J. Mink, "A study of the beam waveguide resonator," Ph.D. dissertation, University of Wisconsin, Madison, 1964.
- [4] R. F. Harrington, *Time-Harmonic Electromagnetic Fields*. New York: McGraw-Hill, 1961, p. 319.
- [5] J. Mink, "Higher modes in electromagnetic wave beams," M.S. thesis, University of Wisconsin, Madison, 1962, p. 59.
- [6] C. G. Montgomery, *Technique of Microwave Measurements* (MIT Radiation Lab. Series, vol. 11). New York: McGraw-Hill, 1947, pp. 58-69.
- [7] A. A. Maryott and F. Buckley, *Table of Dielectric Constants and Electric Dipole Moments of Substances in the Gaseous State*, NBS Circular 537, June 25, 1953.

## Some Characteristics of Alternating Gradient Optical Transmission Lines

WILLIAM H. STEIER, MEMBER, IEEE

**Abstract**—The effect of adding a negative lens between each pair of positive lenses of an optical transmission line is calculated. The negative lens reduces the ability of the transmission line to control the direction of the light beam. The changes in dominant mode spot size, allowed bending radius, critical bend periodicity, and sensitivity to random lateral lens displacements are computed for all ranges of lens spacings and focal lengths which are stable.

#### INTRODUCTION

IN SOME of the proposed light guidance methods which use gas or schlieren-type lenses it may be necessary to consider a system made of alternately positive and negative focal length lenses. For example, if tubular thermal gradient gas lenses [1]-[4] are used, which employ a continuous stream of gas flowing through them, it will be necessary to cool the gas periodically. The region where the gas is cooled will constitute a negative lens of possibly different power from the positive lens [5]. It is of interest, therefore, to consider how the periodic introduction of this negative lens affects the ability of the light guide to control the direction of the light beam.

In this paper, the effect of adding divergent lenses

between each pair of positive lenses of a light guide will be considered. The changes in beam spot size, allowed bending radius of the guide, and stability of the guide to lateral lens displacements are calculated for any ratio of positive to negative lens power. Miller [6] previously calculated the stability conditions and some optimum design parameters for alternate gradient focusing when the power of the positive lenses and the power of the negative lenses are equal.

#### BEAM SPOT SIZE

Consider the transmission line shown in Fig. 1. A negative lens of focal length  $-f/\alpha$  is placed between each pair of positive lenses of focal length  $f$ . The positive lenses are spaced  $2\beta f$ .

The properties of the dominant Gaussian mode of this transmission line can be analyzed by the ray matrix technique of Kogelnik [7]. The ray matrix is the transformation matrix for ray position and slope between the input and output planes. If the input plane is just to the right of a positive lens and the output plane is just to the right of the next positive lens, the ray matrix is

$$\begin{vmatrix} \beta\alpha + 1 & \beta f(2 + \beta\alpha) \\ \frac{\alpha(1 - \beta) - 1}{f} & 1 + \beta(\alpha - 2 - \beta\alpha) \end{vmatrix} = \begin{vmatrix} A & B \\ C & D \end{vmatrix}.$$

Manuscript received November 26, 1965; revised January 19, 1966.  
The author is with the Bell Telephone Laboratories, Inc., Holmdel, N. J.